A typical synthesis procedure was as follows: Step 1: An amorphous mesoporous aluminum containing silica (Si/Al = 100/1) was synthesized using $SiCl_4$ and $AlCl_3$ in ethanol, as in ref. [3]. The surfactant-containing mesoporous solid products were recovered and air-dried at room temperature. Step 2: the dried surfactant-containing mesoporous precursor was impregnated with a 10 wt% solution of TPAOH (free from inorganic alkali). The Si/TPAOH ratio was 8/1. After aging at room temperature, the solid was heated at 60°C to eliminate water, and dried under vacuum for about 24 h at room temperature. Finally, the solid was transferred into a Teflon-lined autoclave and heated at 130°C for different lengths of time. It is considered that the quantity of water adsorbed on the solid plays an important role in the crystallization process. Therefore, the partly crystalline solid was further crystallized at the same temperature for a given time after introducing a small amount of water. Because the solid-state crystallization continues in the presence of this small amount of water, the above process permits control of the crystallinity and the mesopore size of the solid materials. The products were washed with distilled water, dried in air at 80°C, and finally calcined at 550°C for 6 h to remove the organics.

Characterization: Powder XRD patterns of the materials were recorded on a Philips X-ray diffractometer (PW 1010 generator and PW 1050 computer-assisted goniometer) using nickel-filtered $Cu_{K\alpha}$ ($\lambda = 1.5406$ Å) radiation, 0.025° step size and a 1 s step time. Nitrogen adsorption and desorption isotherms at -196°C were established using an Omnisorp-100 apparatus. The specific surface area (S_{BET}) was determined from the linear part of the BET equation ($P/P_0 = 0.05 - 0.15$). The micropore size distribution was calculated from argon adsorption isotherms with the Horváth–Kawazoe method. The calculation of the mesopore-size distribution was performed using the desorption branch of the N_2 adsorption/desorption isotherms and the BJH formula. The mesopore surface area (S_{BJH}) and mesopore volume (V_{BJH}) were obtained from the pore-size distribution curves. The average mesopore diameter, d_p, was calculated as $4V_{BJH}/S_{BJH}$. Although its accuracy is limited, the BJH method, which is still universally utilized in the mesoporous molecular sieves (MMS) literature yields results that are comparable with the current literature values. High-resolution TEM images were obtained on a JEOL 200 CX transmission electron microscope operated at 120 kV. The samples for TEM were prepared by dispersing the fine powders of the products in a slurry in ethanol onto honeycomb carbon copper grids. Solid-state ^{27}Al and ^{29}Si MAS NMR spectra were recorded at room temperature on a Bruker ASX 300 spectrometer.

[1] a) C. T. Kresge, M. E. Leonowicz, W. J. Roth, J. C. Vartuli, J. S. Beck, *Nature* **1992**, *359*, 710–712; b) J. S. Beck, J. C. Vartuli, W. J. Roth, M. E. Leonowicz, C. T. Kresge, K. D. Schmitt, C. T.-W. Chu, D. H. Olsen, E. W. Sheppard, S. B. McCullen, J. B. Higgins, J. L. Schlenker, *J. Am. Chem. Soc.* **1992**, *114*, 10834–10843.

[2] a) D. Zhao, J. Feng, Q. Huo, N. Melosh, G. H. Fredrickson, B. F. Chmelka, G. D. Stucky, *Science* **1998**, *279*, 548–552; b) D. Zhao, Q. Huo, J. Feng, B. F. Chmelka, G. D. Stucky, *J. Am. Chem. Soc.* **1998**, *120*, 6024.

[3] P. Yang, D. Zhao, D. I. Margolese, B. F. Chmelka, G. D. Stucky, *Nature* **1998**, *396*, 152.

[4] A. Corma, *Chem. Rev.* **1995**, *95*, 559.

[5] a) D. Trong On, P. N. Joshi, S. Kaliaguine, *J. Phys. Chem.* **1996**, *100*, 6743; b) E. Dumitriu, D. Trong On, S. Kaliaguine, *J. Catal.* **1997**, *170*, 150.

[6] a) D. Trong On, S. M. J. Zaidi, S. Kaliaguine, *Microporous Mesoporous Mater.* **1998**, *22*, 211; b) D. Trong On, M. P. Kapoor, P. N. Joshi, L. Bonneviot, S. Kaliaguine, *Catal. Lett.* **1997**, *44*, 171.

[7] K. R. Kloetstra, H. W. Zandbergen, J. C. Jansen, H. van Bekkum, *Microporous Mater.* **1996**, *6*, 287.

[8] A. Karlsson, M. Stocker, R. Schmidt, *Microporous Mesoporous Mater.* **1999**, *27*, 181.

[9] L. Huang, W. Guo, P. Deng, Z. Xue, Q. Li, *J. Phys. Chem. B* **2000**, *104*, 2817.

[10] a) A. Corma, V. Fornes, S. B. Pergher, T. L. M. Maesen, J. G. Buglass, *Nature* **1998**, *396*, 353; b) A. Corma, U. Diaz, M. E. Domine, V. Fornes, *J. Am. Chem. Soc.* **2000**, *122*, 2804.

[11] K. R. Kloetstra, H. van Bekkum, J. C. Jansen, *Chem. Commun.* **1997**, 2281.

[12] Y. Liu, W. Zhang, T. J. Pinnavaia, *J. Am. Chem. Soc.* **2000**, *122*, 8791.

[13] R. Ravishankar, C. Kirschhock, B. J. Schoeman, P. Vanoppen, P. J. Grobet, S. Storck, W. F. Maier, J. A. Martens, F. C. De Schryver, P. A. Jacobs, *J. Phys. Chem. B* **1998**, *102*, 2633.

[14] S. A. Bagshaw, E. Prouzet, T. J. Pinnavaia, *Science* **1995**, *269*, 1242.

[15] R. Ryoo, J. M. Kim, C. H. Ko, C. H. Shin, *J. Phys. Chem.* **1996**, *100*, 17718.

[16] R. Borade, A. Sayari, A. Adnot, S. Kaliaguine, *J. Phys. Chem.* **1990**, *94*, 5989.

[17] Y. Liu, W. Zhang, T. J. Pinnavaia, *Angew. Chem.* **2001**, *113*, 1295; *Angew. Chem. Int. Ed.* **2001**, *40*, 1255.

[18] Z. Zhang, Y. Han, L. Zhu, R. Wang, Y. Yu, S. Qiu, D. Zhao, F.-S. Xiao, *Angew. Chem.* **2001**, *113*, 1298; *Angew. Chem. Int. Ed.* **2001**, *40*, 1258.

A Redox Switch Based on Dihydro[5]helicene: Drastic Chiroptical Response Induced by Reversible C−C Bond Making/Breaking upon Electron Transfer**

Jun-ichi Nishida, Takanori Suzuki,* Masakazu Ohkita, and Takashi Tsuji

Helicenes are a special series of chiral molecules with huge optical activities, and thus attract considerable attention for use as nonlinear optical (NLO) materials and asymmetric catalysts.[1] Chiroptical photoswitches that function by modulating the helical geometries of helicenes by light have also been constructed.[2] However, the electron-transfer (ET) reaction of chiral helicenes has not been reported although they can serve as novel "electrochiroptical" transducers when redox-active groups are incorporated. We have found that dihydro[5]helicenes **1** which contain two electron-donating spiro rings undergo reversible C−C bond breaking to give

[*] Prof. Dr. T. Suzuki, Dr. J. Nishida,[+] Dr. M. Ohkita, Prof. Dr. T. Tsuji
Division of Chemistry
Graduate School of Science
Hokkaido University, Sapporo 060-0810 (Japan)
Fax: (+81) 11-746-2557
E-mail: tak@sci.hokudai.ac.jp

[+] Present address:
Department of Electronic Chemistry, Interdisciplinary School of Science and Engineering, Tokyo Institute of Technology
Yokohama 226-8502 (Japan)

Supporting information for this article is available on the WWW under http://www.angewandte.com or from the author.

binaphthylic dications 2^{2+} (Scheme 1). Furthermore, drastic changes of circular dichroism (CD) occurred during the interconversion between optically active **1** and 2^{2+}, thus demonstrating a new entry into the rare chiroptical redox switches.[3]
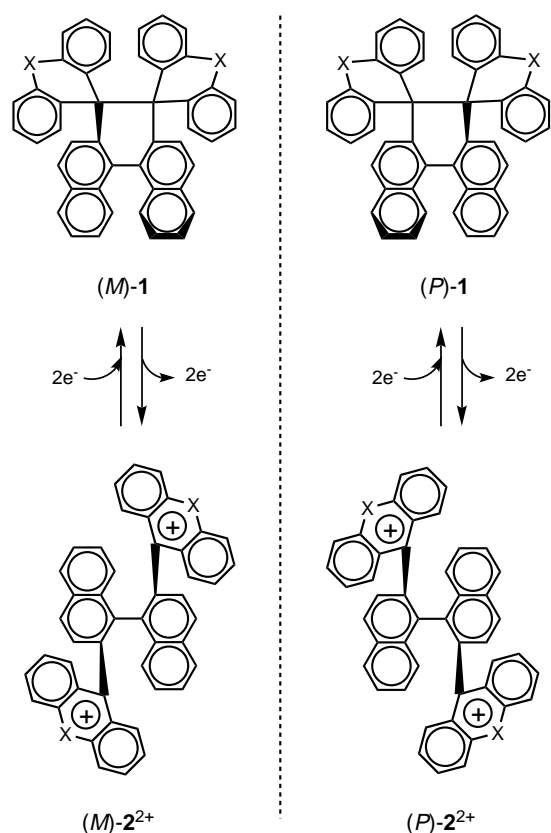
Scheme 1. Interconversion between chiral dihydro[5]helicene **1** and the binaphthylic 2^{2+}; **1a**, $2a^{2+}$ X = S, **1b**, $2b^{2+}$ X = O.

Diols **3a**[4] and **3b**[4] were prepared in 55 and 62% yield, respectively, by the reaction of 2,2′-dilithiobinaphthyl[5] with thioxanthone or xanthone. Deeply colored salts $2a^{2+}(BF_4^-)_2$

3a: X = S
3b: X = O
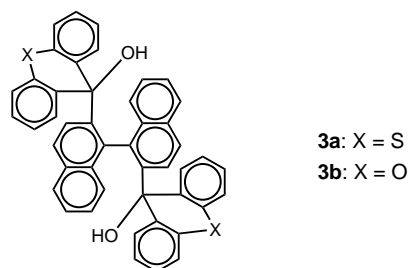
and $2b^{2+}(BF_4^-)_2$[4] were obtained in 96 and 97% yield, respectively, by treating these diols with HBF$_4$ in (EtCO)$_2$O. The single-crystal X-ray analysis on $2a^{2+}(BF_4^-)_2$ shows that the distance between the two methylenium carbon atoms is 3.53 Å (Figure 1a);[6] reduction with zinc led to formation a very long C−C bond between these methylenium carbon atoms (1.651(6) Å for **1a**; Figure 1b) to afford bridged 1,1′-
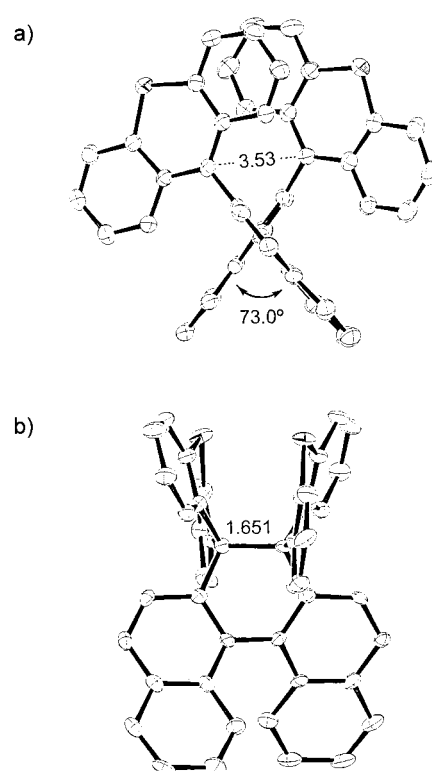

Figure 1. a) Molecular structure of $2a^{2+}$. The dication has a pseudo-C_2 symmetry and the molecular halves in $2a^{2+}$ are twisted by 73.0° around the binaphthyl axis. The two cationic planes overlap in a face-to-face manner (interplanar distance 3.36 Å; dihedral angle 4.5°). b) Molecular structure of **1a**. The dihedral angle between two naphthalene units is 37.1°.

binaphthyls **1a**[4] and **1b**[4] in 92 and 96% yield, respectively. Oxidation of **1a** and **1b** with 2 equivalents of (p-BrC$_6$H$_4$)$_3$N$^+$·SbCl$_6^-$ led to fission of the weak C−C bond to regenerate the dications $2a^{2+}$ and $2b^{2+}$, which were isolated as SbCl$_6^-$ salts in 89 and 81% yield, respectively. The high-yield interconversion between **1** and 2^{2+} indicates that they constitute "reversible" redox pairs, in which the bond making/breaking are induced upon ET. Furthermore, dynamic structural change upon ET causes a large separation of redox potentials of **1** and 2^{2+} (Figure 2, Table 1), thus endowing the present system with high electrochemical bistability.[7]

Optical resolution was carried out by transforming $2a^{2+}$, $2b^{2+}$ into pairs of neutral, diastereomeric ethers (P)-**4a**, **b**[4, 8] and (M)-**5a**, **b**[4, 8] with (R)-1,3-butanediol in the presence of pyridine. The absolute configurations of the binaphthyl moieties were determined by X-ray analyses of (P)-**4a** and (M)-**5b**.[6] By treating these ethers with HBF$_4$ then zinc, chiral dihydro[5]helicenes (P)- and (M)-**1** which have relatively large optical rotations because of their helicene-type structure were prepared (Table 2). Resolved **1a**, **b** and $2a^{2+}$, $2b^{2+}$ show no indication of racemization at room temperature.

The electrochemical response was examined by UV/Vis spectroscopy. As shown in Figure 3a, on interconversion, the redox pairs exhibit electrochromism with a vivid color change; the helicenes **1** show absorption only in the UV region, whereas for the dicationic dyes 2^{2+} the absorption bands occur in the visible region (Table 2). The isosbestic
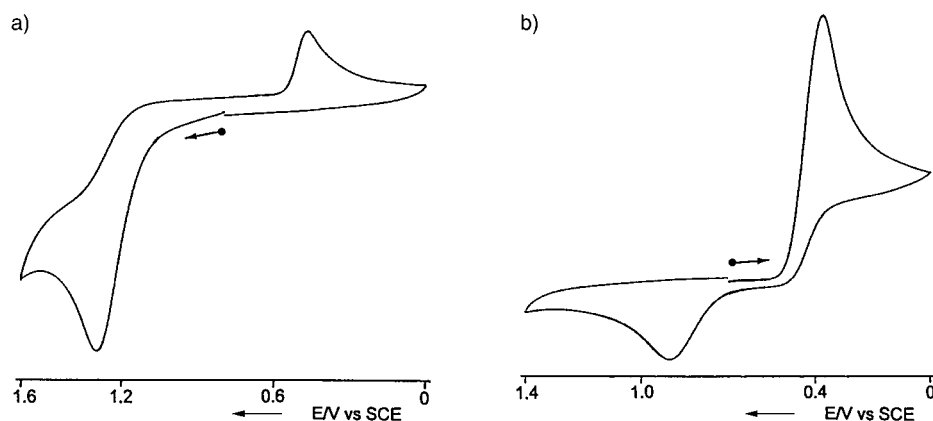
a)

b)

Figure 2. a) Cyclic voltammogram of **1b** in CH_2Cl_2. The reduction peak at $+0.46$ V was absent when the voltammogram was first scanned in the cathodic direction. b) Cyclic voltammogram of **2a^{2+}**$(BF_4^-)_2$ in CH_2Cl_2. The oxidation peak at $+0.93$ V was absent when the voltammogram was first scanned in th eanodic direction. Voltammograms were measured under the conditions shown in Table 1; SCE $=$ standard calomel electrode.

Table 1. Redox potentials of **1** and **2^{2+}**$(BF_4^-)_2$.[a]

	E_p^{ox}	E_p^{red}
1a	$+0.93$ V	
1b	$+1.30$ V	
2a^{2+}		$+0.37$ V
2b^{2+}		$+0.46$ V

[a] Peak potentials in Volts versus SCE; solvent: CH_2Cl_2; electrolyte: $0.1\ mol\,dm^{-3}$ nBu$_4$NBF$_4$; Pt electrode, scan rate 100 mV s^{-1}. Voltammograms were unchanged on measurement at a scan rate of 500 mV s^{-1}.
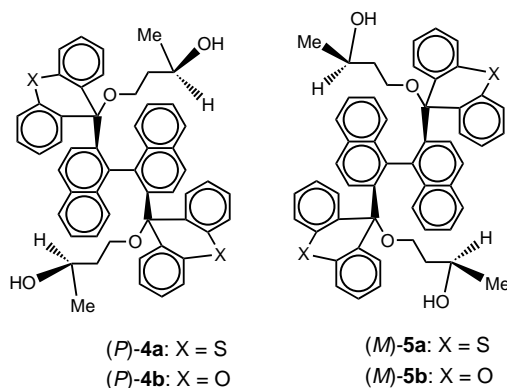

(*P*)-**4a**: X = S
(*P*)-**4b**: X = O

(*M*)-**5a**: X = S
(*M*)-**5b**: X = O

Table 2. Optical rotation for **1**, UV/Vis and CD data for **1** and **2a^{2+}**$(BF_4^-)_2$.

$[\alpha]_D^{27}$ (*c*) in CHCl$_3$: (*P*)-**1a**: $+677°(0.50)$; (*M*)-**1a**: $-678°(0.58)$; (*P*)-**1b**: $+642°(0.16)$; (*M*)-**1b**: $-634°(0.62)$.

UV/Vis λ_{max} (lgε) in MeCN: **1a**: 358 sh (4.01), 345 (4.08), 266 (4.65), 219 nm (4.97); **1b**: 358 (3.99), 344 (4.03), 291 (4.08), 255 (4.69), 219 nm (4.98); **2a^{2+}**$(BF_4^-)_2$: 551 sh (3.86), 516 (3.92), 388 (4.33), 288 (4.92), 227 nm (5.02); **2b^{2+}**$(BF_4^-)_2$: 502 sh (3.86), 382 (3.91), 382 (4.60), 263 (4.77), 225 nm (5.06).

CD λ ($\Delta\varepsilon$) in MeCN: (*P*)-**1a**: 381 (-0.76) 364 ($+4.75$), 336 (-11.4), 303 ($+33.0$), 270 ($+82.0$), 250 nm ($+91.1$); (*M*)-**1a**: 381 ($+0.83$) 364 (-4.68), 336 (-11.5), 303 (-32.1), 270 (-79.4), 250 nm (-89.1); (*P*)-**1b**: 338 ($+14.3$), 305 (-8.27), 264 ($+96.8$), 227 nm ($+137$); (*M*)-**1b**: 338 (-13.4), 305 ($+9.31$), 264 (-93.1), 227 nm (-140); (*P*)-**2a^{2+}**$(BF_4^-)_2$: 503 (-19.0), 394 (-30.7), 362 ($+11.4$), 288 (-120), 261 ($+49.3$) 227 nm ($+231$); (*M*)-**2a^{2+}**$(BF_4^-)_2$: 503 ($+19.3$), 394 ($+30.6$), 362 (-10.9), 288 ($+121$), 261 (-47.2), 227 nm (-227); (*P*)-**2b^{2+}**$(BF_4^-)_2$: 466 (-17.1), 388 (-85.6), 355 ($+43.3$), 275 ($+11.7$), 255 (-44.6) 225 nm ($+180$); (*M*)-**2b^{2+}**$(BF_4^-)_2$: 466 ($+17.1$), 388 ($+85.2$), 355 (-42.4), 275 (-10.8), 255 ($+46.9$) 225 nm (-180).

points observed in the spectra of these reactions are indicative of clean transformation between **1** and **2^{2+}** as well as of the negligible steady-state concentration of the intermediate radical cations.

When the electrochemical study was conducted by using optically active redox pairs, a novel "electrochiroptical" response was detected as shown by the drastic change in the CD spectrum (Figure 3b). Upon electrochemical oxidation of helicene (*P*)-**1a** to (*P*)-**2a^{2+}**, negative ellipticity grows gradually in the long-wavelength region up to 640 nm. The $\Delta\varepsilon$ value at 290 nm changes by as much as

a)

b)
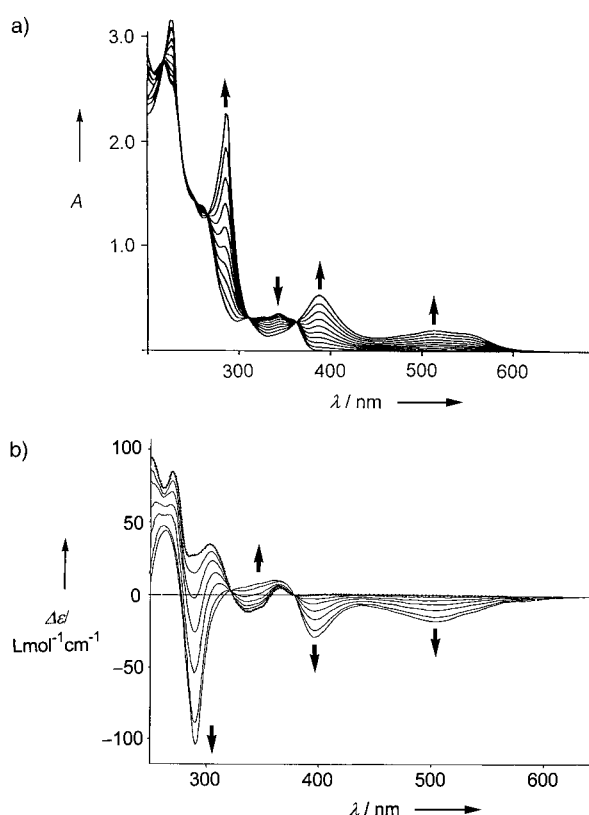

Figure 3. a) Continuous change in the UV/Vis spectrum of **1a** (3.0 mL; $2.96 \times 10^{-5}\ mol\,dm^{-3}$ in MeCN containing $0.05\ mol\,dm^{-3}$ nBu$_4$NBF$_4$) upon constant-current electrochemical oxidation (26 μA) at 10 min intervals. b) Continuous change in the CD spectrum of (*P*)-**1a** (3.0 mL; $3.90 \times 10^{-5}\ mol\,dm^{-3}$ in MeCN containing $0.05\ mol\,dm^{-3}$ nBu$_4$NBF$_4$) upon constant-current electrochemical oxidation (26 μA) at 10 min intervals. The dotted line indicates the spectrum before electrolysis.

$140\ mol^{-1}\,dm^3\,cm^{-1}$. Moreover, presence of isosbestic points (322, 378 nm) indicates the clean interconversion for the chiroptical response.

To conclude this is the first example of chiral helicenes where helicity and the axial chirality of biaryls are reversibly interconverted in a process controlled by external inputs.

Further studies of chiroptical redox switches based on this novel approach are now in progress.

[1] T. J. Katz, *Angew. Chem.* **2000**, *112*, 1997; *Angew. Chem. Int. Ed.* **2000**, *39*, 1921.

[2] W. F. Jager, J. C. de Jong, B. de Lange, N. P. M. Huck, A. Meetsma, B. L. Feringa, *Angew. Chem.* **1995**, *107*, 346; *Angew. Chem. Int. Ed. Engl.* **1995**, *34*, 348; N. Koumura, R. W. J. Zijlstra, R. A. van Delden, N. Harada, B. L. Feringa, *Nature* **1999**, *401*, 152; N. P. M. Huck, W. F. Jager, B. de Lange, B. L. Feringa, *Science* **1996**, *273*, 1686.

[3] C. Westermeier, H.-C. Gallmeier, M. Komma, J. Daub, *Chem. Commun.* **1999**, 2427; G. Beer, C. Niederalt, S. Grimme, J. Daub, *Angew. Chem.* **2000**, *112*, 3385; *Angew. Chem. Int. Ed.* **2000**, *39*, 3252; L. Zelikovich, J. Libman, A. Shanzer, *Nature* **1995**, *374*, 790.

[4] All new compounds gave satisfactory spectral and analytical date, see the Supporting information.

[5] A. Miyashita, H. Takaya, T. Souchi, R. Noyori, *Tetrahedron* **1984**, *40*, 1245.

[6] Crystal structural analyses: **1a**: $C_{46}H_{28}S_2$, $M = 644.85$, orthorhombic, $Pca2_1$, $a = 15.299(4)$, $b = 12.793(3)$, $c = 16.329(4)$ Å, $V = 3196(2)$ Å^3, ρ_{calcd} ($Z = 4$) $= 1.340$ g cm^{-3}. $Rw = 0.048$. **2a**$^{2+}$(BF$_4^-$)$_2$: $C_{46}H_{28}S_2B_2F_8$, $M = 818.45$, monoclinic, Cc, $a = 15.543(3)$, $b = 13.0890(7)$, $c = 18.6698(5)$ Å, $\beta = 107.097(1)°$, $V = 3630.4(7)$ Å^3, and ρ_{calcd} ($Z = 4$) $= 1.497$ g cm^{-3}. $Rw = 0.038$. (P)-**4a**: $C_{54}H_{46}S_2O_4$, $M = 823.08$, orthorhombic, $P2_12_12_1$, $a = 18.2025(6)$, $b = 23.5707(7)$, $c = 9.6503(3)$ Å, $V = 4140.4(2)$ Å^3, and ρ_{calcd} ($Z = 4$) $= 1.320$ g cm^{-3}. $Rw = 0.032$. (M)-**5b** ethanol solvate: $C_{54}H_{46}O_6 \cdot 2 C_2H_6O$, $M = 888.39$, orthorhombic, $P2_12_12$, $a = 22.254(9)$, $b = 23.199(7)$, $c = 9.189(4)$ Å, $V = 4744(2)$ Å^3, and ρ_{calcd} ($Z = 4$) $= 1.236$ g cm^{-3}. $Rw = 0.052$. Crystallographic data (excluding structure factors) for the structures reported in this paper have been deposited with the Cambridge Crystallographic Data Centre as supplementary publication no. CCDC-160767 – 160770. Copies of the data can be obtained free of charge on application to CCDC, 12 Union Road, Cambridge CB21EZ, UK (fax: (+44) 1223-336-033; e-mail: deposit@ccdc.cam.ac.uk).

[7] M. Horner, S. Hünig, *J. Am. Chem. Soc.* **1977**, *99*, 6122; T. Suzuki, J. Nishida, T. Tsuji, *Angew. Chem.* **1997**, *109*, 1387; *Angew. Chem. Int. Ed. Engl.* **1997**, *36*, 1329.

[8] Although chirality of binaphthyl derivatives is commonly designated by (R)/(S), stereochemistry of **2**$^{2+}$, **4**, and **5** is shown by (P) or (M), which indicates that the configuration corresponds to the binaphthyl framework of (P)-**1** or (M)-**1**, respectively.